Charge transfer of multiply charged ions at thermal energies

T. G. Heil, S. E. Butler, and A. Dalgarno
Harvard-Smithsonian Center for Astrophysics, Cambridge, Massachusetts 02138
(Received 13 August 1980)

The charge transfer of N^{2+} and C^{3+} in collisions with atomic hydrogen at thermal energies is studied. Adiabatic molecular eigenfunctions, potential-energy surfaces, and nuclear coupling matrix elements are calculated, and a transformation is effected to a diabatic basis in terms of which the collision problems are solved. The emission characteristics of the spectrum resulting from charge transfer are presented.

I. INTRODUCTION

Depending on the nature of the reactants, charge-transfer reactions of multiply-charged ionic species may proceed rapidly at thermal energies[1] and the ionization structure, the thermal balance, and the emission spectrum of partly ionized plasmas may be substantially influenced by charge transfer recombination and ionization processes. Charge-transfer processes involving multiply charged systems usually lead to specific products which radiate. Thus they are interesting candidates for ultraviolet and x-ray laser systems.

We present here a detailed study of charge-transfer processes involving states of the same molecular symmetry. For each symmetry we selected those adiabatic states for which the radial coupling is significant and transformed them to a diabatic basis. In our diabatic representation the radial coupling matrix elements vanish and transitions between the diabatic states occur through the off-diagonal elements of a potential-energy matrix. The diagonal elements of the potential-energy matrix are diabatic potential-energy surfaces which have the property that they cross in regions where the adiabatic radial coupling is large. Our diabatic basis depends upon the origin of coordinates to which the electronic motion is referred, and we discuss the consequences of different choices of the origin.

To solve the scattering problem in the diabatic formulation, we expanded in eigenfunctions of the total angular momentum and integrated numerically the resulting set of coupled differential equations for the partial waves. We present detailed cross sections as functions of the kinetic energy and analyze the threshold behavior for the charge transfer of N^{2+} and C^{3+} with atomic hydrogen.

II. ADIABATIC AND DIABATIC FORMULATIONS

The Hamiltonian, H, of a system of two nuclei A and B with masses M_A and M_B, respectively, separated by a vector $\vec{R}$ and N electrons with position vectors $\vec{r}_i$ measured from the center of mass of the nuclei, is given in atomic units by

$$H=-\frac{1}{2\mu}\nabla_R^2+T+V=-\frac{1}{2\mu}\nabla_R^2+H_{el}\,, \tag{1}$$

where

$$T=-\frac{1}{2m}\sum_{i=1}^{N}\nabla_i^2-\frac{1}{2M}\sum_{i\neq j}\vec{\nabla}_i\cdot\vec{\nabla}_j\,, \tag{2}$$

V is the sum of the Coulomb interactions of the electrons and the nuclei, $M=M_A+M_B$, $\mu=M_AM_B/M$, and $m=M/(1+M)$. In practice we ignore the small-mass polarization term in (2).

We expand the scattering wave function at energy E in terms of adiabatic electronic eigenfunctions $\psi_i^a(\vec{r}|R)$, determined with the nuclei fixed at R according to

$$\psi(\vec{r},\vec{R})=\sum_i \psi_i^a(\vec{r}|\vec{R})F_i^a(\vec{R})=\vec{\psi}^a\vec{F}^a\,. \tag{3}$$

In the adiabatic representation, the electronic Hamiltonian H_{el} is diagonal so that

$$\langle\psi_i^a(\vec{r}|R)|H_{el}|\psi_j^a(\vec{r}|R)\rangle=\epsilon_i(R)\delta_{ij}\,, \tag{4}$$

where $\langle\cdots\rangle$ denotes an integration over the electronic coordinate space. Then $\vec{F}^a(\vec{R})$ satisfy the set of coupled differential equations

$$\left(-\frac{1}{2\mu}\nabla_R^2\vec{I}-\vec{\epsilon}(R)+E\vec{I}+\frac{1}{2\mu}[2\vec{A}(\vec{R})\cdot\nabla_R+\vec{B}(\vec{R})]\right)F^a(\vec{R})=0\,, \tag{5}$$

where $\vec{I}$ is the unit matrix, $\vec{\epsilon}(R)$ is the diagonal matrix with elements given by Eq. (4), and $\vec{A}(\vec{R})$ and $\vec{B}(\vec{R})$ are the matrices with elements

$$\vec{A}(\vec{R})_{ij}=\langle\psi_i^a|\nabla_R|\psi_j^a\rangle\,, \tag{6}$$

$$\vec{B}(\vec{R})_{ij}=\langle\psi_i^a|\nabla_R^2|\psi_j^a\rangle\,, \tag{7}$$

which couple the adiabatic states and cause transitions between them.[2] If the adiabatic basis $\vec{\psi}^a$ is complete,[3]

$$\vec{B}=\vec{A}^2+\nabla_R\vec{A}\,. \tag{8}$$

The set of equations (5) can be put in a form more convenient for numerical solution by transforming to a diabatic basis. There exists a considerable literature on such transformations which has been comprehensively reviewed by Garrett and Truhlar.[2] Several detailed studies have been made of the two-state case.[4] The three-state case has been investigated by Top and Baer[5] and Baer, Drolshagen, and Toennies.[6] We consider multistate cases and transform to a diabatic representation called the P-diabatic representation by Delos and Thorson.[7]

We restrict attention to couplings between molecular states of the same symmetry and define a new set of nuclear wave functions $\vec{F}^d(\vec{R})$ by the relationship

$$\vec{F}^a(\vec{R})=\vec{C}(R)\vec{F}^d(\vec{R})\,, \tag{9}$$

where

$$\frac{d\vec{C}}{dR}+\vec{A}\vec{C}=0\,. \tag{10}$$

Then

$$\left[-\frac{1}{2\mu}\nabla_R^2\vec{I}-\vec{V}(R)+E\vec{I}+\frac{1}{2\mu}C^{-1}\left(\vec{B}-\frac{d\vec{A}}{dR}-\vec{A}^2\right)\vec{C}\right]\vec{F}^d(\vec{R})=0\,, \tag{11}$$

where $\vec{V}(R)$ is a potential-energy matrix

$$\vec{V}(R)=\vec{C}^{-1}(R)\vec{\epsilon}(R)\vec{C}(R)\,. \tag{12}$$

If we assume that (8) is obeyed, Eq. (11) reduces to

$$\left(-\frac{1}{2\mu}\nabla_R^2\vec{I}-\vec{V}(R)+E\vec{I}\right)\vec{F}^d(\vec{R})=0\,. \tag{13}$$

Equation (13) may be obtained directly from (3) by using the alternative expansion

$$\psi(\vec{r},\vec{R})=\sum_i \psi_i^a(\vec{r}\,|R)F_i^a(\vec{R})=\vec{\psi}^a\vec{F}^d\,. \tag{14}$$

The diabatic and adiabatic electron eigenfunctions $\vec{\psi}^d$ and $\vec{\psi}^a$ are related by

$$\vec{\psi}^d=\vec{\psi}^a\vec{C}\,, \tag{15}$$

and $\vec{\psi}^d$ are such that

$$\left\langle\psi_i^a\left|\frac{d}{dR}\right|\psi_j^a\right\rangle=0\,. \tag{16}$$

The statement can be generalized: If $\vec{\phi}$ is any set and $\vec{a}$ is the matrix with elements $a_{ij}=\langle\phi_i\,|\,d/dR\,|\,\phi_j\rangle$, the set $\vec{\phi}^d=\vec{\phi}\vec{c}$, where

$$\frac{d\vec{c}}{dR}+\vec{a}\vec{c}=0 \tag{17}$$

is such that the matrix of d/dR is the null matrix.

For a complete set, $\vec{\phi}$ must reduce to functions which are, apart from phase factors, independent of R (Ref. 8) and the diabatic basis will then be of little utility. However a diabatic basis constructed by the transformation of a finite set of functions selected to reflect the essential features of the physical system will retain those features and provide an alternative description of them while affecting a considerable simplification in the numerical procedures.

The transformation matrix $\vec{C}(R)$ and the diabatic basis set $\vec{\phi}^d(R)$ depend upon the choice of the origin with respect to which the electron coordinates are held fixed when the radial derivative is taken. Any point $\vec{R}_0$ lying on the line joining the heavy nucleus at $\vec{R}_A$ to the light nucleus at $\vec{R}_B$ may be defined by a parameter η according to

$$\vec{R}_0=\eta\vec{R}_A+(1-\eta)\vec{R}_B\,. \tag{18}$$

Then the matrix elements of $\partial/\partial R$ for two coordinate origins η and η' are related by

$$\left\langle\psi_i^a\left|\frac{\partial}{\partial R}\right|\psi_j^a\right\rangle_{\vec{R}_0}=\left\langle\psi_i^a\left|\frac{\partial}{\partial R}\right|\psi_j^a\right\rangle_{\vec{R}_0'}+(\eta-\eta')\langle\psi_i^a\,|\,\nabla_r\,|\,\psi_j^a\rangle\,, \tag{19}$$

where $\vec{r}_i-\vec{R}_0$ and $\vec{r}_i-\vec{R}_0'$, respectively, are held fixed as the derivatives are taken.

The ambiguity in the scattering formulation which arises from the dependence on coordinate origin expressed in (19) stems from the failure of the theory to describe correctly the translation of the electrons as the atomic systems separate, a defect that leads to spurious couplings which become particularly evident at large internuclear distances. Bates and McCarroll[9] resolved the difficulty by introducing traveling orbitals, and their original study has stimulated a large number of investigations, among the most recent being those of Crothers and Hughes,[10] Delos and Thorson,[7] Hatton, Lane, and Winter,[11] Schmid,[12] Schmalz, Stechel, and Light,[13] and Winter and Hatton.[14]

A natural choice for the origin, consistent with Eqs. (5) and (13), is the center of mass of the nuclei. With this choice, a spurious long-range coupling occurs between the exit channels. The coupling of the exit channels has little effect on the total charge-transfer cross sections but we chose to avoid possible difficulties by using as the origin for the evaluation of $\vec{C}(R)$ the location of the heavy nucleus defined by $\eta=1$. Because we are treating the collision of a heavy ion with atomic hydrogen, the center of mass lies close to the heavy nucleus A. The matrix element $\langle\psi_i^a\,|\,\nabla_r\,|\,\psi_j^a\rangle$ is small compared to $\langle\psi_i^a\,|\,\partial/\partial R\,|\,\psi_j^a\rangle_{\vec{R}_A}$

so that Eq. (19) shows that the coupling matrix elements will differ little for the two origins.

III. NUMERICAL PROCEDURES

A. Potential-energy surfaces and coupling matrix elements

Adiabatic electronic eigenfunctions $\vec{\psi}^a(R)$ and potential-energy surfaces $\vec{\epsilon}(R)$ were calculated by standard configuration-interaction methods. The basis sets were chosen to avoid biasing any particular channel[15] and should be adequate as a description of the scattering states participating in the charge-transfer process.

The Hellman-Feynman theorem enables us to express the adiabatic coupling matrix element in the form

$$\left\langle \psi_i^a \left| \frac{\partial}{\partial R} \right| \psi_j^a \right\rangle = (\epsilon_j^a - \epsilon_i^a)^{-1} \left\langle \psi_i^a \left| \frac{\partial V}{\partial R} \right| \psi_j^a \right\rangle . \tag{20}$$

For $\eta = 1$,

$$\frac{\partial V}{\partial R} = Z_b \sum_{i=1}^{N} \frac{z_{iB}}{r_{iB}^3} , \tag{21}$$

z_{iB} is the z component of $\vec{r}_{iB} = \vec{r}_i - \vec{R}_B$ and Z_b is the nuclear charge on B.

Computer programs exist for the evaluation of the matrix elements of (21). The resulting values are sensitive to the details of the eigenfunctions in the vicinity of the hydrogen nucleus, a region where we expect our configuration-interaction methods to achieve high accuracy.[16]

The adiabatic coupling matrix elements vary rapidly in the neighborhood of avoided crossings. A detailed description of the regions of avoided crossing is needed for the accurate determination of the diabatic states. We found it convenient to interpolate through the crossing region using the simple functions

$$f_{ij}(R) = (\epsilon_i^a - \epsilon_j^a)^2 \left\langle \psi_i^a \left| \frac{\partial}{\partial R} \right| \psi_j^a \right\rangle \tag{22}$$

which change smoothly and slowly.[16]

B. Transformation matrix

To solve Eq. (10) for the transformation matrix $\vec{C}(R)$ we adopted a procedure outlined by Gantmacher.[17] A similar method has been described by Baer.[18] Any solution Eq. (10) such that $\vec{C}(0) = \vec{Q}$ where $\vec{Q}$ is arbitrary, may be expressed in the form

$$\vec{C}(R) = \vec{C}_m(R)\vec{Q} , \tag{23}$$

where $\vec{C}_m(R)$ is the solution which satisfies the boundary condition $\vec{C}(0 = L)$

For our purposes it is convenient to use solutions which satisfy the boundary condition

$$\lim_{R\to\infty} \vec{C}(R) = \vec{I} \tag{24}$$

so that the diabatic basis is identical asymptotically to the adiabatic basis. Then we must have

$$\vec{C}(0) \equiv \lim_{R\to\infty} \vec{C}_m^{-1}(R) = \vec{C}_m^{-1} , \tag{25}$$

for example. We note that for certain choices of η, the limit in Eq. (25) does not exist. If the states are connected asymptotically by a dipole-allowed transition the radial coupling tends to a constant and a diabatic representation is not appropriate without the inclusion of translational factors. If we divide the internal $[0, R]$ into n segments $[R_k, R_{k-1}]$ and define $\Delta R_k = R_k - R_{k-1}$, the solution of Eq. (10) which satisfies the condition (26) is given by

$$C(R) = \exp[-\vec{A}(R_n)\Delta R_n] \exp[-\vec{A}(R_{n-1})\Delta R_{n-1}]$$

$$\times \cdots \exp[-\vec{A}(R_1)\Delta R_1]\vec{C}_m^{-1} + O(\Delta R_k)^2 . \tag{26}$$

In expression (26), the step size may be varied. Each factor involves the exponentiation of a matrix which can be affected either by diagonalization of the matrix $\vec{A}(R_k)\Delta R_k$ or by using a truncated series expansion of the exponential function.

In the cases under study, our electronic basis sets consist of not more than four states and the exact representation of $\exp[-\vec{A}(R_k)\Delta R_k]$ requires at most a third-order polynomial. Because $\vec{A}$ is skew symmetric, the characteristic values are easily determined and Sylvester's theorem[19] may be applied to construct the polynomial representation.

We find that for the four-state case, the exponential of the matrix $\vec{a} \equiv -\vec{A}(R_i)\Delta R_i$ may be written

$$\exp(\vec{a}) = \frac{1}{(\zeta_2^2 - \zeta_1^2)} \left[(\zeta_2^2 \cos\zeta_1 - \zeta_1^2 \cos\zeta_2)\vec{I} + \left(\zeta_2^2 \frac{\sin\zeta_1}{\zeta_1} - \zeta_1^2 \frac{\sin\zeta_2}{\zeta_2} \right) \vec{a} + (\cos\zeta_1 - \cos\zeta_2)\vec{a}^2 + \left(\frac{\sin\zeta_1}{\zeta_1} - \frac{\sin\zeta_2}{\zeta_2} \right) \vec{a}^3 \right] , \tag{27}$$

where

$$\zeta_1 = [\alpha - (\alpha^2 - \beta^2)^{1/2}]^{1/2} \tag{28}$$

and

$$\zeta_2 = [\alpha + (\alpha^2 - \beta^2)^{1/2}]^{1/2} , \tag{29}$$

and α and β may be expressed in terms of the elements a_{ij} of the matrix $\vec{a}$ according to

$$\alpha = \tfrac{1}{2} \sum_{i<j}^{4} a_{ij}^2 , \tag{30}$$

$$\beta = (a_{12}a_{34} - a_{13}a_{24} + a_{14}a_{23})^2 . \tag{31}$$

For the three-state case,

$$\zeta_1 = 0, \ \zeta_2 = (a_{12}^2 + a_{12}^2 + a_{23}^2)^{1/2} \tag{32}$$

and $\exp(\vec{a})$ is represented by

$$\exp(\vec{a}) = \vec{I} + \frac{\sin\zeta_2}{\zeta_2}\vec{a} + \frac{1}{\zeta_2^2}(1 - \cos\zeta_2)\vec{a}^2 . \tag{33}$$

For the two-state case, $\zeta_2 = a_{12}$ and

$$\exp(\vec{a}) = \cos\zeta_2 \vec{I} + \frac{1}{\zeta_2}\sin\zeta_2 \vec{a} = \begin{pmatrix} \cos\zeta_2 & \sin\zeta_2 \\ -\sin\zeta_2 & \cos\zeta_2 \end{pmatrix} . \tag{34}$$

For the two-state case, it follows that

$$\vec{C}(R) = \begin{pmatrix} \cos\zeta(R) & \sin\zeta(R) \\ -\sin\zeta(R) & \cos\zeta(R) \end{pmatrix} , \tag{35}$$

where

$$\zeta(R) = \int_R^\infty A_{12}(R')\,dR' . \tag{36}$$

Having determined $\vec{C}(R)$, the potential-energy matrix $\vec{V}(R)$ in Eq. (13) is readily evaluated from Eq. (12).

C. Scattering equations

To solve Eq. (13) we followed the conventional procedures and expanded $F_j^d(\hat{R})$ in an orthonormal set of total angular momentum wave functions $D_{\Lambda M}^J(\hat{R})$, where J is the total angular momentum quantum number, M is its projection quantum number, Λ is the projection quantum number of the electronic orbital angular momentum onto the internuclear axis, and $\hat{R}$ specifies the orientation in space of the internuclear axis. Thus

$$\vec{F}^d(\hat{R}) = \sum_{JM} (-)^J \left(\frac{(2J+1)}{4\pi}\right)^{1/2} D_{\Lambda M}^J(\hat{R})\vec{f}^J(R)/R . \tag{37}$$

The radial partial wave functions $\vec{f}^J(R)$ satisfy for each J the coupled differential equations

$$\left(\frac{d^2}{dR^2} + 2\mu E - \frac{J(J+1) - \Lambda^2}{R^2}\right)\vec{I}\vec{f}^J(R) - 2\mu\vec{V}(R)\vec{f}^J(R) = 0 . \tag{38}$$

In calculations we took $\Lambda = 0$. Then for the incoming channel i, $f_i^J(R)$ satisfies the boundary condition at large R that

$$f_i^J(R) \sim k_i^{-1/2}\{\exp[-i(k_iR - \tfrac{1}{2}J\pi)] - S^J(i,i)\exp[i(k_iR - \tfrac{1}{2}J\pi]\} , \tag{39}$$

where

$$k_i^2 = 2\mu[E - V_{ii}(\infty)] . \tag{40}$$

For the exit channels, $f_f^J(R)$ satisfy the boundary conditions appropriate to scattering by a repulsive Coulomb potential:

$$f_f^J(R) \sim -k_f^{-1/2}S^J(i,f) \times \exp i(k_fR - \gamma k_f^{-1}\ln 2k_fR + \sigma_f - \tfrac{1}{2}J\pi) , \tag{41}$$

where σ_f is the Coulomb scattering phase shift, $\gamma = \mu ZZ'$ where Z and Z' are the asymptotic ionic charges, and

$$k_f^2 = 2\mu[E - V_{ff}(\infty)] . \tag{42}$$

Equations (39) and (40) define the scattering matrix $S^J(i,f)$ in terms of which the cross section may be written

$$\sigma_{if}(E) = \frac{\pi g_i}{k_i^2}\sum_J (2J+1)|S^J(i,f)|^2 , \tag{43}$$

where g_i is the probability that the initial approach occurs in the corresponding molecular symmetry. The total charge-transfer cross section is the sum of Eq. (43) over the molecular symmetry states, i, formed by the initial approach and for each symmetry over the possible final states, f:

$$\sigma(E) = \sum_{i,f}\sigma_{if}(E) . \tag{44}$$

To solve Eq. (38) numerically we used the log-derivative algorithm of Johnson[20] with the asymptotic matching procedure generalized to include both Ricatti-Bessel and Coulomb functions.[21]

IV. POTENTIAL-ENERGY SURFACES

We have carried out calculations for the charge-transfer reactions

$$N^{2+}(2s^2 2p^2 P^0) + H - N^+ + H^+ \tag{45}$$

and

$$C^{3+}(2s^2 S) + H - C^2 + H^+ . \tag{46}$$

For reaction (45), the adiabatic potential-energy surfaces $\vec{\epsilon}(R)$ and eigenfunctions $\vec{\psi}^a(R)$ have been

calculated.[15] Avoided crossings were found between the incoming $^3\Pi$ state of NH^{2+} and the outgoing $^3\Pi$ state which dissociates into $N^+(2s2p^3\,^2D^0)$ and H^+. The potential-energy curves are presented in Fig. 1. They undergo two avoided crossings, an outer one in the vicinity of $R = 6.3a_0$ and an inner one near $3.1a_0$. The outer avoided crossing is accessible at zero energy but not the inner.

The adiabatic coupling matrix element $A_{12}(R)$ is shown in Fig. 2. It is small everywhere except in the regions of the avoided crossings where it undergoes rapid variations, described approximately by Lorentzian profiles.[22] The transformation parameter $\zeta(R)$ is illustrated in Fig. 3. It is small until the avoided crossing region is entered and then increases to a value of about 1.4 after which it decreases as R passes through the region of the second avoided crossing, the contributions from the two crossings almost canceling. Such behavior is expected if at each avoided crossing the mixing of the two states merely interchanges their character and orbital variations are negligible.[16,22,23]

The behavior of $\zeta(R)$ is reflected in that of the diabatic curves included in Fig. 1. In contrast to the adiabatic curves, the diabatic curves cross in the regions of strong adiabatic coupling. After crossing they tend to merge again with the adiabatic curves.

The coupling matrix element $V_{12}(R)$ connecting the two $^3\Pi$ diabatic states is shown in Fig. 4. It varies slowly with R and is everywhere small.

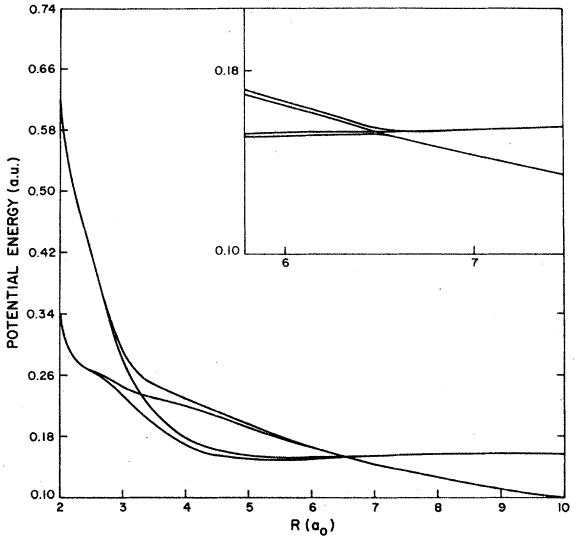

FIG. 1. The adiabatic and diabatic potential-energy curves of the $2\,^3\Pi$ and $3\,^3\Pi$ states of NH^{2+}. The inset shows the crossing region near $6.5a_0$ on a larger scale. The diabatic curves lie inside the adiabatic and cross twice.

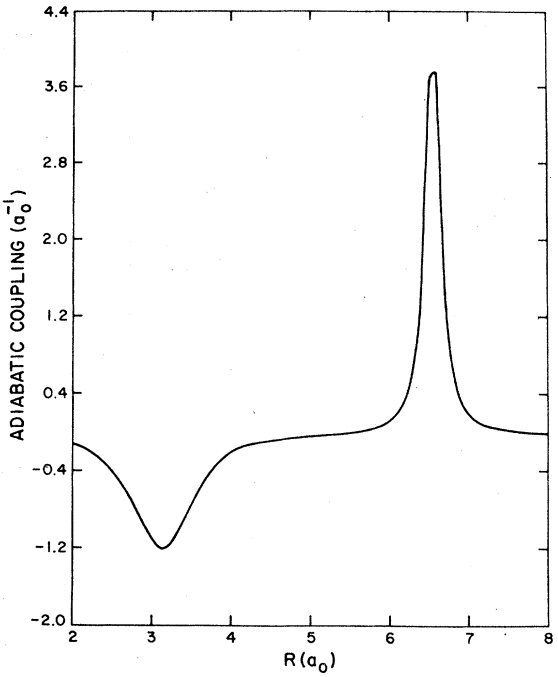

FIG. 2. The adiabatic coupling matrix element connecting the $2\,^3\Pi$ and $3\,^3\Pi$ states on NH^{2+}.

The diabatic states are weakly coupled and the diabatic representation provides a more accurate zero-order description of the collision process.

We have carried out similar calculations for reaction (46). The adiabatic potential surfaces show

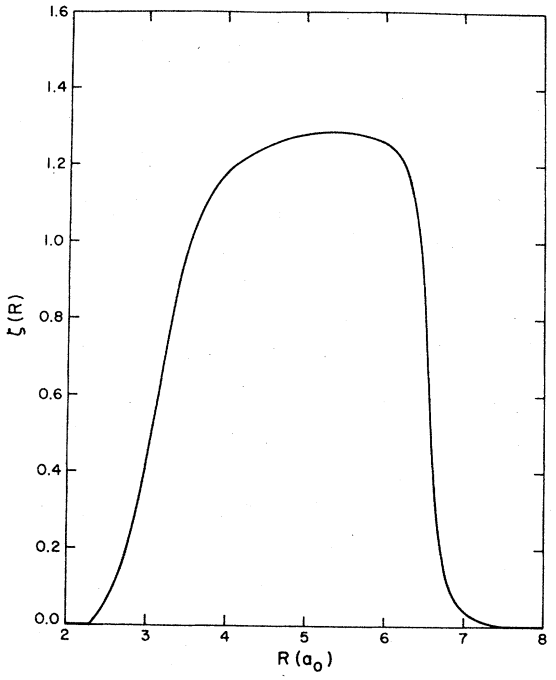

FIG. 3. The diabatic transformation parameter $\zeta(R)$ for the $2\,^3\Pi$ and $3\,^3\Pi$ states of NH^{2+}.

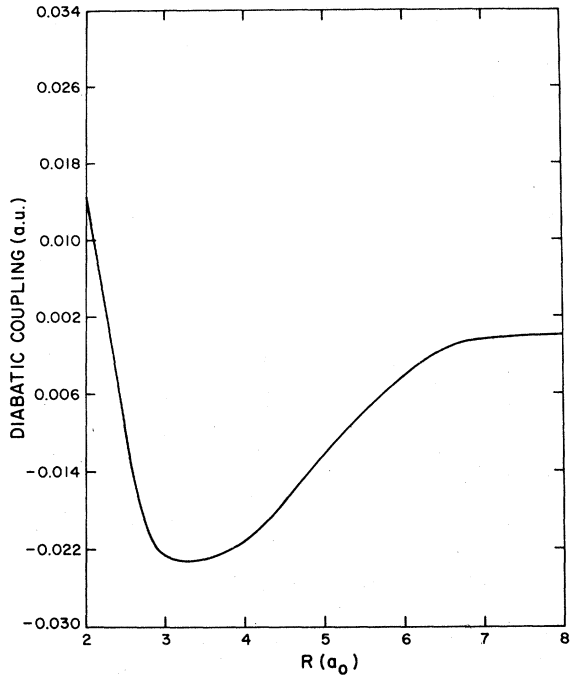

FIG. 4. The diabatic coupling matrix element connecting the $2\,^3\Pi$ and $3\,^3\Pi$ states of NH^{2+}.

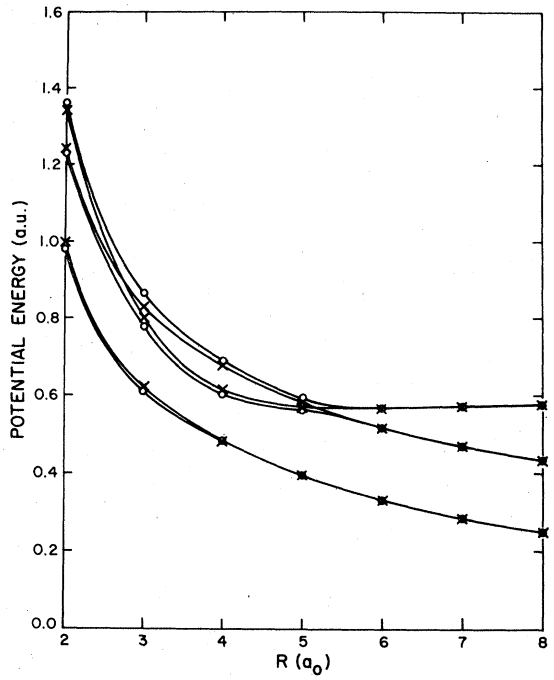

FIG. 5. The adiabatic and diabatic potential-energy curves for the $1^1\Sigma^+$, $2^1\Sigma^+$, and $3^1\Sigma^+$ states of CH^{3+}: o-adiabatic, × -diabatic.

avoided crossings in the $^1\Sigma^+$ and $^3\Sigma^+$ molecular symmetries and do so in each symmetry for two final states. The $^1\Sigma^+$ states dissociate to $C^{2+}(2p^2\,^1S)$ and H^+ and to $C^{2+}(2p^2\,^1D)$ and H^+, and the $^3\Sigma^+$ states dissociate to $C^{2+}(2s3s\,^3S)+H^+$ and $C^+(2s3p\,^3P^0)+H^+$.

The calculated surfaces for the $^1\Sigma^+$ states are presented in Fig. 5. Avoided crossings occur at nuclear separations near $5.2a_0$ and $2.5a_0$ for the charge-transfer channels. The avoided crossings are more apparent in the variation of the adiabatic coupling matrix elements with R, shown in Fig. 6. The coupling between the initial channel and one of the final channels is strong and similar in behavior to the NH^{2+} case. The other couplings are

TABLE I. Charge-transfer cross sections $\sigma(E)$ in units of 10^{-16} cm^2 as a function of relative energy E in eV for $N^{2+}+H \rightarrow N^+ + H^+$.

Energy (eV)	$\sigma(E)$ N^{2+}
2.7×10^{-4}	30.2
2.7×10^{-3}	83.0
2.7×10^{-2}	27.3
0.27	10.1
1.5	5.1
3.9	4.2
8.1	3.0

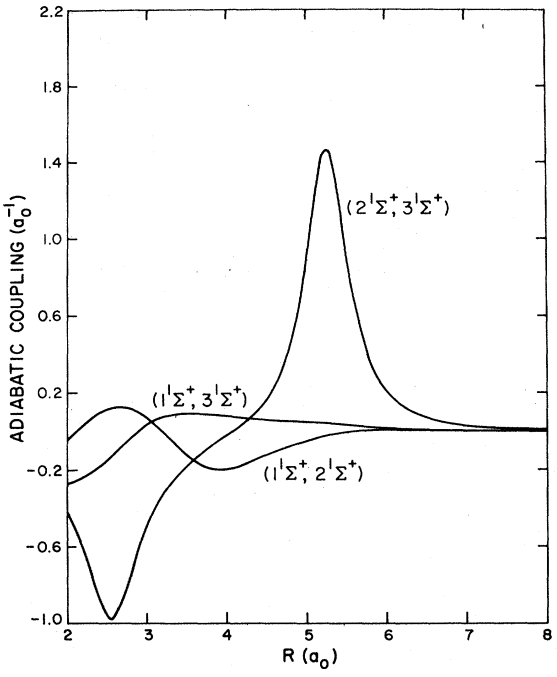

FIG. 6. The adiabatic coupling matrix elements between the $1^1\Sigma^+$, $2^1\Sigma^+$, and $3^1\Sigma^+$ states of CH^{3+}.

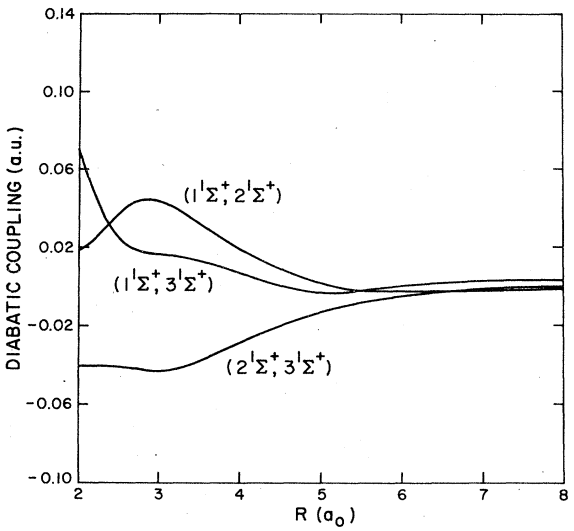

FIG. 7. The diabatic coupling matrix elements between the $1^1\Sigma^+$, $2^1\Sigma^+$, and $3^1\Sigma^+$ states of CH^{3+}.

weak.

The diabatic potential-energy surfaces are included in Fig. 5. The strongly coupled pair of states produce diabatic curves which cross at their outer approach and cross back again in the inner region. The weakly coupled states produce a diabatic curve which differs little from the adiabatic. The diabatic coupling matrix elements are presented in Fig. 7. They are everywhere small and the diabatic states are weakly coupled, so much so that the distorted-wave approximation would suffice to describe the scattering.

TABLE II. Charge-transfer cross sections $\sigma(E)$ in units of 10^{-16} cm^2 as a function of relative energy E in eV for $C^{3+}+H \rightarrow C^{2+}+H^+$.

	$\sigma(E)$			
Energy (eV)	$C^{2+}(2p^2\,^1S)$	$(2p^2\,^1D)$	$(2s3s\,^3S)$	$(2s3p\,^3P^0)$
0.27	1.8	4.4×10^{-5}	35.3	
1.5	2.0	4.7×10^{-5}	20.4	6.9×10^{-2}
3.9	2.6	5.8×10^{-5}	15.3	3.3×10^{-2}
8.1	3.4	1.2×10^{-4}	12.0	5.8×10^{-2}

The calculated potential-energy surfaces for the $^3\Sigma^+$ states of CH^{3+} are given in Fig. 8. An avoided crossing of the potential-energy curve of the $^3\Sigma^+$ entrance channel occurs with that of the nearest $^3\Sigma^+$ exit channel near $5.2a_0$ and with that of the other exit channel near $11a_0$.

The diabatic potential-energy curves, also given in Fig. 8, reflect the occurrence of the two single crossings. They lie inside the adiabatic curves, and after each crossing they merge with the interchanged adiabatic curves.

The adiabatic and diabatic coupling matrix elements are shown in Figs. 9 and 10, respectively.

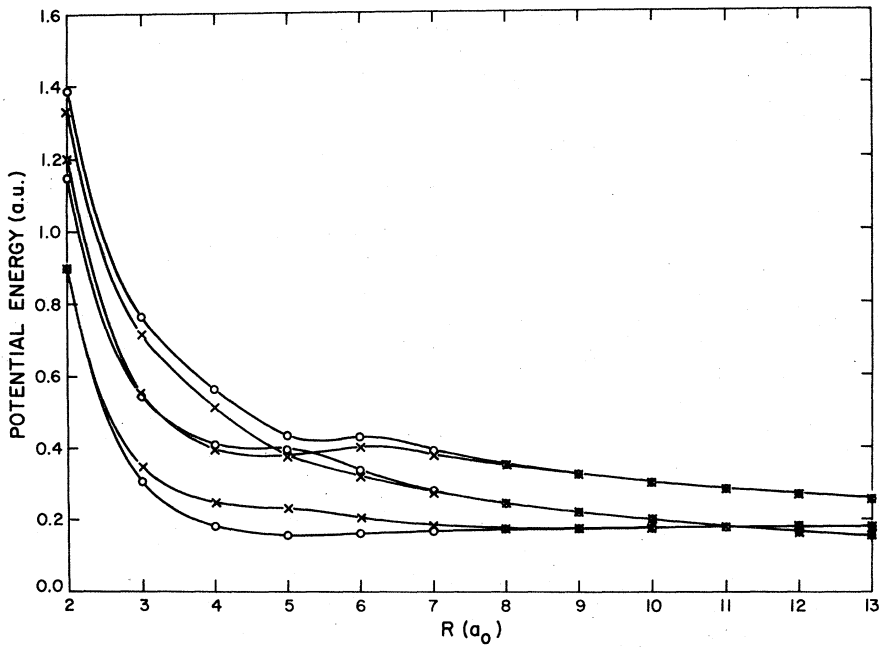

FIG. 8. The adiabatic and diabatic potential-energy curves for the $1^3\Sigma^+$, $2^3\Sigma^+$, and $3^3\Sigma^+$ states of CH^{3+}: o-adiabatic, x-diabatic.

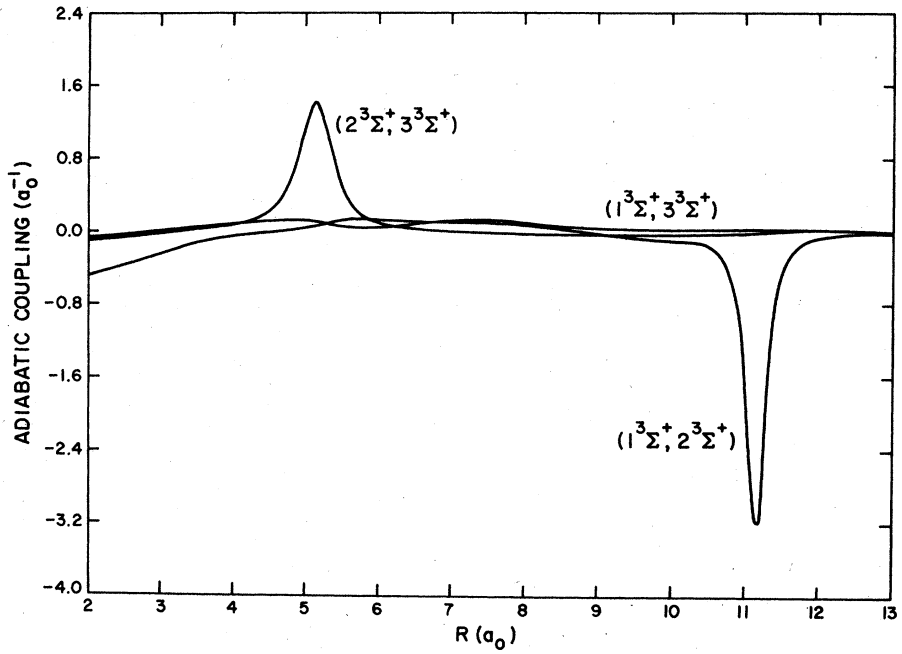

FIG. 9. The adiabatic coupling matrix elements between the $1^3\Sigma^+$, $2^3\Sigma^+$, and $3^3\Sigma^+$ states of CH^{3+}.

The adiabatic elements vary rapidly in the neighborhood of the avoided crossings and the diabatic elements are relatively smooth and small in magnitude.

The calculated cross sections for reaction (45) are listed in Table I for relative energies up to 8 eV. The outer avoided crossing is accessible at zero energy, and at low velocities the scattering is controlled by the long-range polarization attraction. The cross sections initially decrease

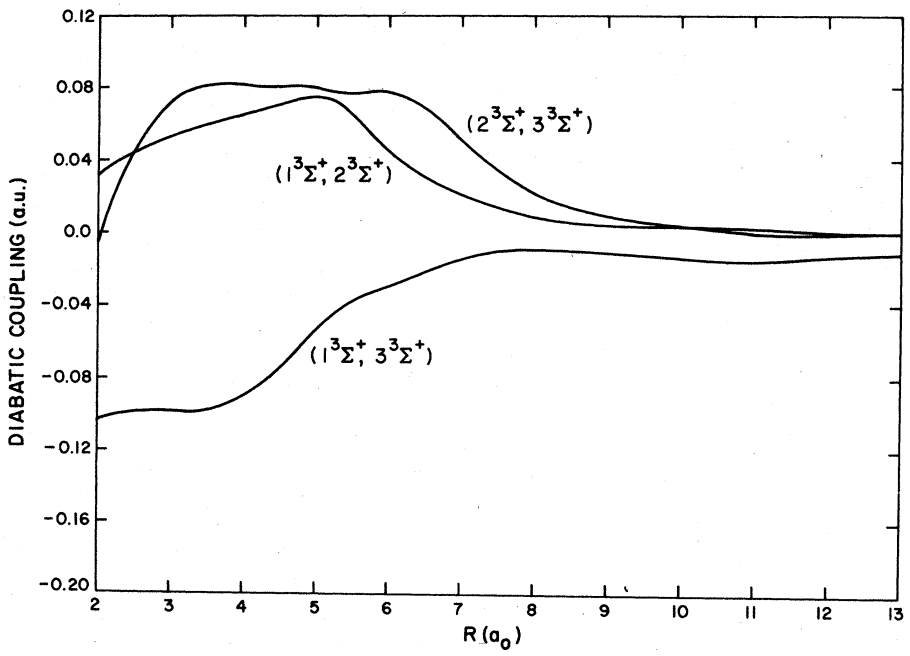

FIG. 10. The diabatic coupling matrix elements between the $1^3\Sigma^+$, $2^3\Sigma^+$, and $3^3\Sigma^+$ states of CH^{3+}.

TABLE III. Rate coefficients, k, for the charge-transfer recombination of N^{2+} and C^{3+} in neutral atomic hydrogen as a function of the kinetic temperature T.

	$k(10^{-9}$ cm^3 s$^{-1})$		
T(K)	$N^{2+}(2s2p^3\,^2D^0)$	$C^{3+}(2p^2\,^1S)$	$C^{3+}(2s3s^3S)$
5×10^3	0.78	0.19	2.88
10^4	0.86	0.29	3.26
2×10^4	0.97	0.49	3.71
3×10^4	1.05	0.71	4.04
5×10^4	1.11	1.05	4.38

approximately as the inverse of the velocity of relative motion, deviations arising from the occurrence of shape resonances. At higher velocities, the influence of the polarization force diminishes and the cross section increases with increasing energy after passing through a minimum. At some higher energy beyond the range of our calculations it will decrease again. Charge transfer of C^{3+} with H at low energies produces C^{2+} ions in the $(2p^2\,^1S)$, $(2p^2\,^1D)$, $(2s3s\,^3S)$, and $(2s3p\,^3P^0)$ states. The individual cross sections are listed in Table II for energies of relative motion up to 8 eV.

The cross sections for the reactions leading to $C^{2+}(2p^2\,^1S)$ and $C^{2+}(2s3s\,^3S)$ have a similar behavior to those for the reactions of N^{2+} with H. The outer crossings are accessible at zero energy and the cross sections initially decrease approximately as the inverse of the relative velocity before passing through a minimum and increasing towards higher energies. Eventually they will also decrease.

Cross sections for the reaction leading to $C^{2+}(2s3s\,^3S)$ have been obtained earlier by Blint, Watson and Christensen[24,25] based upon approximate direct calculations of the diabatic coupling matrix $\vec{V}$. The agreement with our results is satisfactory at low velocities though significant differences are developing at the upper limit of our energy range which require further study.

The cross sections for transfer into channels dissociating to $C^{2+}(2p^2\,^1D)$ and $C^{2+}(2s3p\,^3P^0)$ are small. The relevant avoided crossings are inaccessible at zero energy and the cross sections tend exponentially to zero at low velocities. Shape resonances cause deviations from a smooth curve. The magnitudes of the cross sections vary directly as the square of the coupling matrix elements and are unreliable.

The thermally averaged rate coefficients are presented in Table III. They are large and charge transfer is an important recombination process in multiply ionized plasmas.[26] The charge transfer of N^{2+} preferentially populates the $(2s2p^3\,^3D^0)$ state with the emission of photons at wavelengths near 1085 Å. The charge transfer of C^{3+} with H preferentially populates the $(2p^2\,^1S)$ and $(2s3s\,^3S)$ states of C^{2+}. The $(2p^2\,^1S)$ state decays to the $(2s2p\,^1P^0)$ state with the emission of a photon at 1247 Å and the $(2s3s\,^3S)$ state decays to the $(2s2p\,^3P^0)$ state with the emission of a photon near 538 Å.

The N II line at 1085 Å and the C III line at 1247 Å have been identified in the averaged solar spectrum.[27] The averaged spectrum contains a line at 538 Å which also appears in the solar-flare spectrum.[28] In both compilations, the line is listed as unidentified. We suggest it is due to the $2s3s\,^3S - 2s2p\,^3P^0$ transition in C III.

ACKNOWLEDGMENTS

We are indebted to Dr. R. McCarroll and Dr. D. S. F. Crothers for useful discussions. This work was supported in part by the Department of Energy under Contract No. DE-AS02-76ER02287.

[1]D. R. Bates and B. L. Moiseiwitsch, Proc. Phys. Soc. London Sect. A 67 , 805 (1954); A. Dalgarno, Proc. Phys. Soc. London Sect. A 67 , 1010 (1954).
[2]B. C. Garrett and D. G. Truhlar, in *Theoretical Chemistry: Advances and Perspectives, Vol. 6A,* edited by D. Hendersen (Academic, New York, 1981), p. 215.
[3]F. T. Smith, Phys. Rev. 179, 111 (1969); B. Andresen and S. E. Nielsen, Mol. Phys. 21 , 523 (1971); V. Sidis and H. Lefebvre-Brion, J. Phys. B 4 , 1040 (1971); V. K. Babamov, J. Chem. Phys. 69 , 3414 (1978).
[4]B. Andresen and S. E. Nielsen, Mol. Phys. 30 , 755 (1975); M. Baer, Chem. Phys. Lett. 35 , 112 (1975); T. R. Dinterman and J. B. Delos, Phys. Rev. A 15 , 463 (1977); M. B. Faist and R. D. Levine, J. Chem. Phys. 64 , 2953 (1977); R. Cimiraglia and M. Persico, Mol. Phys. 38 , 1707 (1979); T. G. Heil and A. Dalgarno, J. Phys. B 12 , L557 (1979); D. S. F. Crothers and N. R. Todd, J. Phys. B 13 , 547 (1980).
[5]Z. H. Top and M. Baer, J. Chem. Phys. 66 , 1363 (1977).
[6]M. Baer, G. Drolshagen, and J. P. Toennies, J. Chem. Phys. 73, 1690 (1980).
[7]J. B. Delos and W. R. Thorson, Phys. Rev. A 18, 117 (1978); A 18, 135 (1978); J. Chem. Phys. 70, 1774 (1979).
[8]H. Gabriel and K. Taulbjerg, Phys. Rev. A 10 , 741 (1974).
[9]D. R. Bates and R. McCarroll, Proc R. Soc. London Ser. A 245 , 175 (1958).
[10]D. S. F. Crothers and J. E. Hughes, Philos. Trans.

R. Soc. London Ser. A 292 , 539 (1979); D. S. F. Crothers and J. G. Hughes, Phys. Rev. Lett. 43 , 1584 (1979).
[11]G. J. Hatton, N. F. Lane, and T. G. Winter, J. Phys. B 12 , L571 (1979).
[12]G. B. Schmid, J. Phys. B 12 , 3909 (1979).
[13]T. G. Schmalz, E. B. Stechel, and J. C. Light, J. Chem. Phys. 70 , 5660 (1979).
[14]T. G. Winter and G. J. Hatton, Phys. Rev. A 21 , 793 (1980).
[15]S. E. Butler, Phys. Rev. A 20 , 2317 (1979).
[16]S. E. Butler, Phys. Rev. A 23, 1 (1981).
[17]F. R. Gantmacher, *The Theory of Matrices*, Vol. II, (Chelsea, New York, 1960), pp. 127–135.
[18]M. Baer, Mol. Phys. (in press).
[19]R. A. Frazer, W. J. Duncan, and A. R. Collar, *Elementary Matrices* (McMillan, New York, 1947), p. 78.
[20]B. R. Johnson, J. Comput. Phys. 13 , 445 (1973).
[21]R. McCarroll and P. Valiron, Astron. Astrophys. 53 , 83 (1976).
[22]M. Oppenheimer, J. Chem. Phys. 57 , 3899 (1972).
[23]R. S. Berry, J. Chem. Phys. 27 , 1288 (1957).
[24]R. J. Blint, W. D. Watson, and R. B. Christensen, Ap. J. 205 , 634 (1976).
[25]W. D. Watson and R. B. Christensen, Ap. J. 231 , 627 (1979).
[26]S. Butler, T. G. Heil, and A. Dalgarno, Ap. J. 241, 442 (1980).
[27]J. E. Vernazza and E. M. Reeves, Ap. J. Suppl. 37 , 485 (1978).
[28]K. P. Dere, Ap. J. 221 , 1062 (1978).